Atmos. Chem. Phys. Discuss., 11, 1333–1366, 2011
www.atmos-chem-phys-discuss.net/11/1333/2011/
doi:10.5194/acpd-11-1333-2011

Atmospheric Chemistry and Physics Discussions

Size-resolved and bulk activation properties of aerosols in the North China plain: the importance of aerosol size distribution in the prediction of CCN number concentration

Z. Z. Deng[1], C. S. Zhao[1], N. Ma[1], P. F. Liu[1], L. Ran[1], W. Y. Xu[1], J. Chen[1], Z. Liang[1], S. Liang[1], M. Y. Huang[1,2], X. C. Ma[2], Q. Zhang[2], J. N. Quan[2], P. Yan[3], S. Henning[4], K. Mildenberger[4], E. Sommerhage[4], M. Schäfer[4], F. Stratmann[4], and A. Wiedensohler[4]

[1]Department of Atmospheric and Oceanic Sciences, School of Physics, Peking University, Beijing, China
[2]Beijing Weather Modification Office, Beijing Meteorological Bureau, Beijing, China
[3]Centre for Atmosphere Watch and Services, Chinese Academy of Meteorological Sciences, China Meteorological Administration, Beijing, China

[4] Leibniz Institute for Tropospheric Research, Leipzig, Germany

Received: 11 December 2010 – Accepted: 31 December 2010 – Published: 18 January 2010

Correspondence to: C. S. Zhao (zcs@pku.edu.cn)

Published by Copernicus Publications on behalf of the European Geosciences Union.

ACPD
11, 1333–1366, 2011

Abstract

Size-resolved and bulk activation properties of aerosols were measured at a regional/suburban site in the North China Plain (NCP), which is occasionally heavily polluted by anthropogenic aerosol particles and gases. A CCN (Cloud Condensation Nuclei) closure study is conducted with bulk CCN number concentration (N_{CCN}) and calculated N_{CCN} based on the aerosol number size distribution and size-resolved activation properties.

The observed N_{CCN} are higher than those observed in other locations than China, with average N_{CCN} of roughly 2000, 3000, 6000, 10 000 and 13 000 cm^{-3} at supersaturations of 0.056, 0.083, 0.17, 0.35 and 0.70%, respectively. An inferred critical dry diameter (D_m) is calculated based on the measured N_{CCN} and aerosol number size distribution assuming homogeneous chemical composition. This inferred cut off diameter varies in a wide range, indicating that it is impossible to predict N_{CCN} with a fixed critical diameter.

Size-resolved activation measurements show that most of the 300 nm particles are activated at the investigated supersaturations, while almost no particles of 30 nm are activated even at the highest supersaturation of 0.72%. The activation ratio increases with increasing supersaturation and particle size. The slopes of the activation curves for ambient aerosols are not as steep as those observed in calibrations with ammonium sulfate suggesting that the observed aerosols is an external mixture of more hygroscopic and hydrophobic particles. This conclusion is confirmed by hygroscopicity measurements performed during two intensive field studies in 2009.

The calculated N_{CCN} based on the size-resolved activation ratio and aerosol number size distribution correlate well with the measured N_{CCN}, and show an average overestimation of 19%. Sensitivity studies of the CCN closure show that the N_{CCN} for each supersaturation is well predicted with the campaign average of size-resolved activation curves. These results indicate that the aerosol number size distribution is critical in the prediction of possible CCN. The N_{CCN} can be estimated with average activation curve,

ACPD
11, 1333–1366, 2011

along with a well described aerosol number size distribution.

1 Introduction

The aerosol impact on cloud and the cloud feedbacks are currently considered as the largest uncertainty in climate system (IPCC, 2007). Great efforts have been made to predict the number concentration of cloud condensation nuclei (CCN) for modeling applications (Boucher and Lohmann, 1995; Khvorostyanov and Curry, 2006). Comparisons of the measured and predicted N_{CCN} can evaluate the measurements and the methods, and present possible parameterization schemes. Closure between the measured and the predicted N_{CCN} is achieved, when the difference between them falls within the uncertainty of the measurements and predictions.

It is well documented that the Raoult and Kelvin effects control the ability of an aerosol particle to be a possible CCN (Rogers and Yau, 1989). The aerosol size distribution and chemical composition are the two most important aerosol properties that could be measured by current technologies. They are often utilized to predict the CCN number concentration (N_{CCN}). Bulk chemical composition of PM_{10} or PM_1 from filter sampling is often used in such closure studies (Bougiatioti et al., 2009), while the knowledge of a size-resolved composition possibly improves the prediction of N_{CCN} (Medina et al., 2007). Stroud et al. (2007) measured chemical composition of aerosols with an aerosol mass spectrometer (AMS). The N_{CCN} was predicted with a kinetic model. CCN were substantially over predicted (by 35.8±28.5%) using size-averaged chemical composition, and by introducing size-dependent chemical composition the closure was improved considerably (average error 17.4±27%).

Measurements of chemical information are time- and resource-consuming, direct and detailed measurement techniques of activation properties are thus urgently required. Size-resolved activation ratios (the fraction of the activated particles in the total aerosol number) are frequently determined in laboratory and field studies. Such methods, described in detail by Frank et al. (2006), are used in instrument calibrations in

ACPD
11, 1333–1366, 2011

laboratory and applied in measurements of aerosol activation properties. Size-resolved activation properties of known compounds, such as water-soluble organic and inorganic substances (Hori et al., 2003; Cruz and Pandis, 1997), mixtures of known compounds (Giebl et al., 2002), and natural mixtures are intensively investigated in laboratory studies.

The relative importance of the variation of the aerosol number size distribution and the chemical composition has been discussed in several studies, validating which of them is more essential in the observation and modeling of CCN. Aerosol chemical composition is more important at lower supersaturations than at higher supersaturations, because the relative change in N_{CCN} induced by the change of aerosol composition is larger for circumstances with low N_{CCN} at lower supersaturations (Kuwata et al., 2005). Particles' ability to act as CCN is largely controlled by aerosol size rather than composition (Dusek et al., 2006). Mixing state also needs to be accounted for (Anttila, 2010; Medina et al., 2007).

Concentrations of pollutants are rapidly increasing in China, especially in the North China Plain (NCP) due to great economic development. As observed from the satellites, the aerosol loading and trace gas concentrations (CO, SO_2, NO_x, etc.) are much higher than those in other places of the world (Xu, et al., 2011). The high aerosol (mass and number) and trace gas concentrations might change the physical and chemical properties of the atmosphere, and cloud physical processes, e.g., the precipitation in North China is decreased significantly during the last 40 yr and the reduction of precipitation is strongly correlated to increasing aerosol concentrations (Zhao et al., 2006).

In an aerosol polluted region, a large number of aerosol particles can be activated at the typical cloud supersaturations in the atmosphere, e.g. 0.05%–1%. These particles have different size and compositions, resulting in different growth times in the activation process. They compete for water vapor to be activated. The larger particles, which may activate first deplete the water vapor, decreases supersaturation and may thus suppress the activation of other smaller particles (Zhao et al., 2005). Soluble trace gases could be absorbed by particles and may lower the equilibrium vapor pressure

ACPD
11, 1333–1366, 2011

(Kulmala et al., 1997).

In this work, the aerosol activation properties in the NCP are investigated, using the aerosol number size distribution, the size-resolved activation ratio, and the bulk N_{CCN}. This work presents a method to better understand the relationship between aerosol number size distribution and N_{CCN}. Finally, a closure study is performed between the measured and calculated N_{CCN} using aerosol size distribution and size-resolved activation ratio.

2 Relationship between aerosol size distribution and CCN number concentration

This section presents the relationship between the aerosol number size distribution and CCN number concentration to help understanding the current work.

The supersaturation required to activate a single aerosol particle (Critical Supersaturation, SS_c) is determined by its size and composition using the Köhler equation. However, it is difficult to obtain the chemical composition for any individual atmospheric aerosol particles.

A bulk CCN number concentration can be measured employing a CCN counter set at a given supersaturation. The CCN is a subset of the total aerosol population. A schematic plot shows the relationship between aerosol number size distribution and CCN in Fig. 2.

Assuming uniform chemical composition throughout the size range, a critical dry particle diameter D_m (pink line in Fig. 2) can be calculated from the measured N_{CCN} and aerosol size distribution. The number concentration of aerosol particles with sizes larger than D_m equals to N_{CCN}.

$$N_{CCN} = \int_{D_m}^{\infty} n\left(\log D_p\right) d\log D_p \quad (1)$$

ACPD
11, 1333–1366, 2011

where D_p is the diameter of aerosol particle, and $n(\log D_p)$ is the function of the aerosol number size distribution.

Atmospheric aerosol particles have complicated size-dependent chemical compositions due to various physical and chemical processes involved. Even at a certain particle size, their chemical composition may be quite different if the aerosol is heterogeneous mixed. For atmospheric aerosol particles with various chemical composition, the CCN concentration ($N_{CCN,Cal}$) can be calculated using the following equation,

$$N_{CCN,Cal} = \int_0^\infty n_{CCN}(\log D_p)\, d\log D_p = \int_0^\infty A(\log D_p)\, n(\log D_p)\, d\log D_p \quad (2)$$

where $n_{CCN}(\log D_p)$ is the CCN number size distribution function, and $A(\log D_p)$ is the size-resolved activation ratio.

The size-resolved activation ratio $A(\log D_p)$ is determined by aerosol particle size and chemical composition. In order to understand the role of size and composition on the size-resolved activation ratio, two extreme conditions for aerosol composition are introduced and discussed here. First, we consider highly soluble particle substance such as a NaCl aerosol. A critical dry diameter D_{NaCl} can be calculated using Köhler equation (blue line in Fig. 2). Particles with sizes smaller than D_{NaCl} cannot be activated at the corresponding supersaturation.

For another extreme case, we consider an insoluble but wettable particle (IBW). Here, a Kelvin diameter (D_{Kelvin}) is determined using the Kelvin equation (green line in Fig. 2). The particles larger than D_{Kelvin} are all activated.

The critical dry diameters of NaCl, $(NH_4)_2SO_4$ and IBW aerosol particles at various supersaturations are shown in Table 1. Typical supersaturation for stratiform clouds, cumulus clouds, and fog are 0.05%, 0.25%–0.8%, and 0.1%, respectively (Seinfeld and Pandis, 2006). Ammonium sulfate particles larger than 34 nm, respectively sodium chloride particles for sizes larger than 26 nm may activate at supersaturation of 0.8%. The size of an IBW particle needs to be above several micrometers to be activated at

ACPD
11, 1333–1366, 2011

very low supersaturations in stratiform clouds. The activation ratio of aerosols is 0 at D_{NaCl} and 1 at D_{Kelvin}. The activation ability of ambient aerosols in the real atmosphere varies between these two extreme cases of highly soluble substance and IBW. In this paper, ambient aerosol activation properties are investigated in field measurements using CCN counter and mobility size spectrometer.

3 Measurements and data processing

3.1 The field site

The NCP underwent a rapid development during the last three decades. Heavy industries and dense population caused severe particulate and gaseous pollutions. Wuqing is a town located in the NCP between the two Megacities of Beijing and Tianjin (Fig. 1). Investigations of the physical and chemical properties of the atmosphere were conducted at that regional/suburban site in Wuqing.

The field study, concerning aerosol activation properties and optical properties of aerosols, were carried out in January 2010. The aerosol number size distribution and the bulk CCN number concentration were measured from 31 December 2009 to 20 January 2010. The size-resolved activation ratios were measured only at daytime.

3.2 Instrumentations

The data used in this work include the aerosol number size distribution, the N_{CCN} and the size-resolved CCN activation ratio. The set-up of instruments is shown in Fig. 3. The ambient aerosol sample passes through a silica gel diffusion drier, maintaining a relative humidity (RH) below 30%. The aerosol sample is then led into the air-conditioned measurement container with a temperature around 20 °C.

Aerosol number size distributions (13.8–750 nm) were obtained by a Scanning Mobility Particle Sizer (SMPS, Model 3936, TSI, USA) with a time resolution of five minutes. The SMPS consist mainly of Differential Mobility Analyzer (DMA, Model 3081)

ACPD
11, 1333–1366, 2011

and Condensation Particle Counter (CPC, Model 3772). The DMA sheath and sample flows were 3 lpm and 0.3 lpm, respectively.

A continuous-flow dual CCN counter (CCN-200) (Roberts and Nenes, 2005; Lance et al., 2006) manufactured by Droplet Measurement Technologies (DMT, USA) was utilized to measure the CCN activation properties. The CCN-200 has two columns to measure different samples at different supersaturations at the same time. One column directly measures the dry polydisperse aerosol sample to obtain the bulk CCN concentration, while the other measures the size-resolved activation properties.

Quasi-monodisperse aerosol particles with diameters of 30, 40, 50, 75, 100, 150, 200 and 300 nm were selected by another DMA. The sheath and sample flow rates were 8 lpm and 0.8 lpm, respectively. The sample flow was then split into two parts, 0.5 lpm for CCN counter and 0.3 lpm for CPC (Model 3776). CCN counter reports the N_{CCN}, and CPC reports the condensation nuclei number concentration (N_{CN}). The activation ratio is defined as the ratio between N_{CCN} and N_{CN}.

Both columns operated at the same supersaturations at the same time. Five supersaturations (nominally 0.07, 0.10, 0.20, 0.40, and 0.80%) made up a cycle of half an hour, taking 10 min for 0.07% and 5 min for other supersaturations. The N_{CCN} for five supersaturations were available every half an hour. The selected size of aerosol particles after the DMA was also changed every 30 min, during which the activation properties at five supersaturations were measured. Particle sizes with number concentrations with less than 10 cm^{-3} were skipped. Activation ratios of all the diameters at five supersaturations were available every 3–4 h depending on the number of selected particle sizes.

The CCN counter was calibrated with ammonium sulfate particles (Rose et al., 2008) before and after the campaign. The critical dry diameters determined from the activation curves of ammonium sulfate, are converted to effective supersaturation (SS_e) utilizing the Köhler equation. The Köhler equation employs the temperature dependent surface tension of water (Cooper and Dooley, 1994), temperature dependent solubility of ammonium sulfate in water (Seinfeld and Pandis, 2006), and molality dependent

ACPD
11, 1333–1366, 2011

van't Hoff factor (Young and Warren, 1992; Low, 1969).

The temperature gradients (TG) and SS_e were linearly fitted. The SS_e of the atmospheric measurement is calculate from the TG with this TG~SS_e relationship. The calibration shows that the effective supersaturations were 0.058, 0.085, 0.18, 0.36 and 0.72% for size-resolved measurements, and 0.056, 0.083, 0.17, 0.35 and 0.70% for bulk measurements.

3.3 Data processing

For each supersaturation, N_{CCN} is recorded every second. To ensure the instrument and data stability, these records are filtered with different criterions of temperature and flow, e.g., the temperatures and flow rates need to be close to the set values. The average N_{CCN} at each supersaturation is computed using the processed records.

The CCN activation ratio is calculated based on both the N_{CCN} and aerosol number concentration (N_{CN}) of quasi-monodisperse aerosol particles. Each aerosol sample consists of aerosol particles with a small range of electrical mobility, due to the DMA transfer function. The particles may however carry different number of electric charges. This means that even for the same mobility, these particles can have different particle sizes. The DMA transfer function width and the multiple charges skew the activation curves.

A multiple charge correction is then applied for the CCN activation ratio without considering the width of DMA transfer function (as the Appendix A). The presence of multiply charged particles, which usually have higher activation ratio than the singly charged particle, induces a falsely higher measured activation ratio for singly charged diameters. The correction will reduce the activation ratio especially for the smaller particle sizes.

ACPD
11, 1333–1366, 2011

4 Results

4.1 Summary of bulk CCN measurements

The statistical results for the particle number concentration (N_a) and N_{CCN} are summarized in Table 2. The particle number concentration ranged from 1000 to 100 000 cm^{-3}. Most of the time, the particle number concentration was however between 10 000 and 40 000 cm^{-3}.

High N_{CCN} were observed during periods of heavy aerosol pollution. The N_{CCN} depended strongly in the different weather systems during the measurement period. The N_{CCN} was found to be as high as 28 000 cm^{-3} at 0.70% supersaturation. Normally, the N_{CCN} was however about 2000, 3000 and 6000 cm^{-3} at supersaturation of 0.056, 0.083 and 0.17%, and more than 10 000 cm^{-3} for supersaturations above 0.35%. On other hand, under meteorological situation especially with strong winds, the N_{CCN} can be as low as around 100 cm^{-3} at supersaturations of 0.056 and 0.083%, and less than 2000 cm^{-3} at 0.7% supersaturation, because the aerosol number concentration in the accumulation mode range becomes relatively low.

The inferred critical diameters D_m, as defined in Eq. (1) in Sect. 2.1, are calculated based on the N_{CCN} and the corresponding aerosol number size distribution. The D_m for each supersaturation varies dramatically (Fig. 4). Variations of D_m for supersaturations above 0.17% are larger than that for 0.056% and 0.083% supersaturations. The D_m are in the ranges of 190–280, 160–260, 95–180, 65–120 and 50–100 for supersaturations of 0.056, 0.083, 0.17, 0.35 and 0.7%, respectively. The average aerosol number concentration within these size ranges are 2000, 2900, 5800, 6900 and 8100 cm^{-3}. These values are comparable to the campaign average N_{CCN}. The predicted N_{CCN} with a fixed critical dry diameter inferred from the measurement might result in relative deviation of nearly 100%. This indicates that it is impossible to predict CCN number concentration from the aerosol number size distribution using a fixed critical dry diameter.

ACPD
11, 1333–1366, 2011

4.2 Size-resolved activation ratio

Figure 5 is the time series of the activation ratio for 75, 100, and 200 nm particles at different supersaturations. As the aerosol is size-selected, the activation ability for one particle size depends on the chemical effects on aerosol activation, including amount of the soluble inorganic matters, slightly soluble organics (Bilde and Svenningsson, 2004), and the surface active compounds (Facchini et al., 1999; Henning et al., 2005). The activation ratio divides the size-selected aerosol particles into more CCN-active and less CCN-active group. The population of these two groups depends on their mixing state and their chemical compositions.

For lower supersaturations and smaller particles, e.g. 75 nm at 0.058 and 0.085% supersaturations, the activation ratios are close to 0, because the particles are too small to be activated. Particles of 75, 100, and 200 nm are mostly activated at supersaturations of 0.36 and 0.72%. It can be seen in Fig. 5 that the activation ratios for 200 nm particles at 0.056 and 0.085%, for 100 nm particles at 0.18%, and for 75 nm particles at 0.36% mainly ranged between 0.2 and 0.8.

Figure 6 is the size-resolved activation curve for each supersaturation averaged for the campaign. The activation curves for ambient aerosols are shown in colored lines. The activation curves at different supersaturations are distinct. Particles smaller than 150 nm are rarely activated at supersaturation 0.058%, while 40 nm particles have activation ratios of 0.4 at 0.72% supersaturation.

Most 300 nm particles are activated at all of the measured supersaturations. Although 300 nm is much smaller than the Kelvin diameter for most of the measured supersaturations (Table 1), small soluble fraction enables the particle to be activated. For example, ammonium sulfate fractions of 18, 8, 2, 0.3 and 0.03% (and the rest is insoluble) are sufficient to activate a 300 nm particle at supersaturations of 0.07, 0.1, 0.2, 0.4 and 0.6%. Almost no particles of 30 nm are activated at the measured supersaturations, because even pure ammonium sulfate particles of 30 nm are unable to be activated at 0.8% supersaturation. The activation ratios are strongly dependent on the

ACPD
11, 1333–1366, 2011

particle size. The activation ratio increases with increasing diameter.

The slope of the activation curves of ammonium sulfate represents internally mixed aerosol (Gray curves in Fig. 6). The slopes for ambient aerosols are not as steep as that of ammonium sulfate, suggesting that the aerosol is chemically and/or morphologically externally mixed (Frank et al., 2006). For each size, hygroscopic growth and activation of particles depend on their chemical components and mixing state. The external mixing is also observed in the hygroscopicity measurements in Wuqing (Liu et al., 2011). And the GF-PDF (Probability Distribution Function of Growth Factor) of a size selected aerosol, in turn, can provide the activation ratio for various supersaturations (Su et al., 2010).

4.3 Calculation of CCN number concentration based on aerosol number size distribution and size-resolved activation ratio

The N_{CCN} can be calculated from the aerosol number size distribution and the size-resolved activation ratios (Eq. 2). The calculation of N_{CCN} using this method is evaluated in this study with parallel measurements of N_{CCN} and size-resolved activation properties (Fig. 7).

The two columns of the CCN counter are independent and they are used for bulk and size-resolved measurement. Both columns are set to the same five supersaturations, nominally 0.07, 0.10, 0.20, 0.40 and 0.80%, during the measurement. However, the calibration shows that the effective supersaturations are different (Sect. 3.2).

The measured N_{CCN} is compared with the calculated N_{CCN} at the same supersaturation in CCN closure study. The measured N_{CCN} and effective supersaturation are fitted with an empirical function

$$N_{CCN} = N_0 \left(1 - e^{-k(S-S_0)}\right), \quad (3)$$

where S is supersaturation, N_0, k and S_0 are fitted parameters.

ACPD
11, 1333–1366, 2011

This function describes the N_{CCN}~S relationship in this study better than $N_{CCN}=CS^k$ suggested by Twomey (1959). If an activation curve is measured at effective supersaturation SS_M, a N_{CCN} at SS_M is achieved by fitting the CCN spectra measured closest in time with the activation curve with Eq. (3). This is referred to as the "measured" N_{CCN}, and then used to be compared with the calculated N_{CCN}.

N_{CCN} can be calculated from the above corrected data with Eq. (2). The calculated N_{CCN} based on the measured aerosol number size distribution and the size-resolved activation ratio, along with the bulk measurement, is shown in Fig. 8a. The calculated N_{CCN} is highly correlated with the measurement (R^2=0.9501). However, the calculation generally overestimates the N_{CCN}. The linear fitted lines have slopes larger than 1 for each supersaturations and 1.169 for all the data.

The difference between measured and calculated N_{CCN} might result from the measurement uncertainties. The uncertainty for aerosol number size distribution is under controlled conditions within 10% (Wiedensohler et al., 2011). The uncertainty for CCN measurements comes from the uncertainty of supersaturation, the water depletion inside the CCNC, and the particle counting and flow rate. The uncertainty of calibrated supersaturation, by comparing the calibration before and after the campaign, is small in this study. The water depletion may occur in the CCN counter in the bulk CCN measurement. The high particle number concentration also may reduce the counting rate of the CCN counter (manual of CCN counter). Taking these sources into account, the uncertainty of bulk and size-selected CCN number concentration might exceed that of aerosol size distribution measurement. Moore et al. (2010) reported uncertainties of 0.17 for N_{CCN}, 0.067 for N_{CN} and thus 18% for activation ratio when the N_{CN} is 100 cm^{-3}. Other uncertainties arise from the coarse size resolution of the activation ratio, the absence of DMA transfer function correction for the activation ratio and the linear interpolation of the activation ratio on the scale of logD_p. The uncertainties are estimated to be >10% for bulk N_{CCN}, and >21% for calculated N_{CCN}. The calculated CCN number concentrations agree well with the measured one within the estimated uncertainties of the measurements and the data processing.

ACPD
11, 1333–1366, 2011

The calculation of N_{CCN} employs the activation ratio curves and the aerosol number size distribution. The activation ratio curves (AR) represent the chemical composition and mixing state of aerosol. The aerosol size distribution can be described with two factors, i.e. the population of aerosol (particle number concentration, Na) and the normalized aerosol size distribution (NASD). To explore the relative importance of these three factors (AR, Na and NASD), sensitivity tests are performed. The N_{CCN} are calculated when one of the above factors is replaced by the average conditions.

The average AR based on 20-day measurements in January 2010 are given in Fig. 6. Figure 8b shows the calculated N_{CCN} utilizing these averaged activation curves and the real-time measurement of aerosol size distribution. There are more scattered data than the base case. The relative bias is larger than the base case and the correlation coefficient (R^2) is lower. Nevertheless, both relative bias and R^2 are close to those of the result using all real-time data. The replacement of the average activation ratio does not cause significant changes to the results. These average size-resolved activation ratio curves provide a good estimation of activation properties.

Figure 8c shows the result when particle number concentrations are fixed to the average one. The aerosol number size distributions are replaced with the product of the NASD and the average particle number concentration. The calculated N_{CCN} for each supersaturation, compared to the base case, converge to narrower range. The N_{CCN} is linearly related to particle number concentration. The calculated N_{CCN} is limited by the prescribed aerosol number concentration. The average relative deviation is larger than the base case and the correlation coefficient is lower. The linear fitted lines have slopes and intercepts highly biased from 1 and 0.

The average NASD is obtained from the average of all normalized aerosol number size distributions. The aerosol number size distribution in the calculation is replaced with the product of the average NASD and the original particle number concentration. Compared to the previous cases, the average NASD case has much more scattered data; both the average relative bias and the average relative deviation are also larger (Fig. 8d).

ACPD
11, 1333–1366, 2011

From the results discussed for Fig. 8c and d, it can be seen that the aerosol number size distribution plays a critical role in calculation of N_{CCN}. The evolution of aerosol number size distribution depends on the sources, coagulation, growth, aging and deposition processes. It is improper to calculate the N_{CCN} with prescribed aerosol size distribution due to its significant variation.

5 Summary

The aerosol-cloud interaction is an essential issue in climate change research. The relationship between aerosol and CCN is complicated, because the aerosols origin from various emissions, and undergo atmospheric physical and chemical processes. Measurements of size-resolved activation gain insight of the ability of aerosol acting as CCN. The bulk and size-resolved activation properties of submicron aerosols were investigated in January 2010 at a regional/suburban site in the NCP.

High aerosol mass and number concentrations are connected with high N_{CCN} in the NCP. The N_{CCN} occasionally exceeds 20 000 cm^{-3} at supersaturations above 0.35% during pollution episodes, while it can be low as several hundred under clean conditions. The average N_{CCN} are roughly 2000, 3000, 6000, 10 000 and 13 000 cm^{-3} at supersaturations 0.056, 0.083, 0.17, 0.35 and 0.70%, respectively. Such high N_{CCN} are also observed in the vicinity of Guangzhou (Rose et al., 2010) and south of Beijing (Wiedensohler et al., 2009).

However, the relationship between this abundant CCN at the surface and the cloud properties is not clear yet. The cloud property is determined by the thermodynamic processes, the available CCN for activation and microphysical processes. Deng et al. (2009) presented the aircraft measurement of cloud droplet number concentration (CDNC) around Beijing. The CDNC are 376±290, 257±226, 147±112, 60±35 and 60±84 cm^{-3}, for cumulus, stratocumulus, altocumulus, altostratus, and nimbostratus clouds, respectively. This observed CDNC around Beijing area are far lower than the surface measured CCN number concentration. Most of the aerosols are trapped inside

ACPD
11, 1333–1366, 2011

the boundary layer. The aircraft measurements show that the aerosol number concentration decreases with height (Liu et al., 2009). Aerosol particles in the boundary layer do not always have opportunity to be activated into the cloud droplets above the boundary layer. There are also some mechanisms to transfer the surface aerosol into the free troposphere, such as convection. Local circulations like mountain valley breeze and sea land breeze may also alter the vertical profiles of aerosol. Chen et al. (2009) shows that the pollutants in the boundary layer can be injected from the planetary boundary layer and form an elevated pollution layer in the free troposphere due to the Mountain Chimney Effect.

The size-resolved activation measurement and CCN closure study provide insight of the detailed activation ability. More than 50% of the particles larger than 200, 170, 90, 70, and 45 nm are activated at supersaturations of 0.058, 0.085, 0.18, 0.36 and 0.72%, respectively. These diameters are a little larger than but close to the critical diameters of ammonium sulfate particles (Table 1). This implies that the aerosols in the North China Plain consist of highly soluble material. Soluble fractions of more than 83% are needed to activate these particles, assuming aerosol composition of ammonium sulfate and an insoluble core. The water soluble organics and the influence of surface tension are also expected to contribute to the activation.

The widths of the activation curves are larger than those in calibration. This indicates that the particles are externally mixed in the perspective of CCN activation. The direct measurements of hygroscopic growth of aerosol using HH-TDMA also show high hygroscopicity and external mixture (Liu et al., 2011).

The size-resolved activation curves, based on the measured aerosol size distributions, provide a method to calculate CCN size distribution and N_{CCN}. Sensitivity studies of this method were performed to explore the relative importance of the size-resolved activation ratio, the aerosol number concentration and normalized aerosol size distribution. The calculated N_{CCN} are highly biased when the aerosol number concentration or normalized aerosol size distribution are fixed to the average level. This shows that both the aerosol number concentration and normalized aerosol size distribution are of great

ACPD
11, 1333–1366, 2011

importance in the prediction of CCN number concentration. An average size-resolved activation ratio is sufficient to describe the activation properties of the aerosols in the NCP. The activation ability of aerosol depends on the solubility, the surface tension and the van't Hoff factor, as well as the size. The variation of aerosol chemical composition affects the solubility, the surface tension and the non-ideality of the solution. But these variations do not necessarily influence the overall activation ratio. The variation of size-resolved activation ratio caused by aerosol chemical composition has weak impacts on bulk aerosol activation. This average activation property and well predicted aerosol size distribution can predict N_{CCN} successfully. These results would help us to understand the role of size and chemical compositions in their activation processes, and enables us to develop an aerosol-CCN scheme based on such size-resolved measurements.

Appendix A

The procedure of multiple charge correction

The aerosol sample selected by DMA is a quasi-mono-disperse aerosol with a width of mobility range and several charges for each particle. A simple multiple charge correction is applied for the CCN activation ratio without consideration of the DMA transfer function. Thus only the central mobility is considered in the aerosol sample.

Assuming the activation ratio for the particle with j charges passing through channel i is A_{ij}, i=1, 2, ..., I, the measured activation ratio can be expressed as

$$M_i = \frac{\sum_{J=1}^{J} N_{\mathrm{CCN}ij}}{\sum_{J=1}^{J} N_{\mathrm{CPC}ij}} = \frac{\sum_{J=1}^{J} A_{ij} N_{\mathrm{CPC}ij}}{\sum_{J=1}^{J} N_{\mathrm{CPC}ij}} = \frac{\sum_{J=1}^{J} A_{ij}\mathrm{MCF}_{ij}}{\sum_{J=1}^{J} \mathrm{MCF}_{ij}} = \sum_{J=1}^{J} A_{ij} F_{ij} \quad \text{(A1)}$$

where J is the maximum number of charges on one particle, here we use 10. $N_{\mathrm{CPC}ij}$ is the number of particles passing through channel i with j charges. It can be calculated from the parallel aerosol size distribution and the charge probability (Wiedensohler, 1988), considering the DMA transfer function.

ACPD
11, 1333–1366, 2011

The relative multiple charge fraction is

$$\mathrm{MCF}_{ij} = N_{\mathrm{CPC}ij}/N_{\mathrm{CPC}i1}, \tag{A2}$$

and

$$F_{ij} = \mathrm{MCF}_{ij}/\sum_{k=1}^{J}\mathrm{MCF}_{ik}. \tag{A3}$$

A_{ij} can be expressed as the linear interpolation of the activation ratios at the measured diameters,

$$\begin{aligned} A_{ij} &= A_{i(j)} + \left(A_{i(j)+1} - A_{i(j)}\right)\frac{\log D_{ij} - \log D_{i(j)}}{\log D_{i(j)+1} - \log D_{i(j)}} \\ &= A_{i(j)}\frac{\log D_{i(j)+1} - \log D_{ij}}{\log D_{i(j)+1} - \log D_{i(j)}} + A_{i(j)+1}\frac{\log D_{ij} - \log D_{i(j)}}{\log D_{i(j)+1} - \log D_{i(j)}} \\ &= A_{i(j)}\frac{\log\left(D_{i(j)+1}/D_{ij}\right)}{\log\left(D_{i(j)+1}/D_{i(j)}\right)} + A_{i(j)+1}\frac{\log\left(D_{ij}/D_{i(j)}\right)}{\log\left(D_{i(j)+1}/D_{i(j)}\right)} \\ &= A_{i(j)}P_{ij} + A_{i(j)+1}Q_{ij} \end{aligned} \tag{A4}$$

where D_{ij} is the diameter of the particles passing through channel i with j charges, $i(j)$ is the index of the largest one among the measured diameters which are smaller than or equals to D_{ij}, A_i indicates the activation ratio of the singly charged particles in the corresponding channels.

When $i(j)$ equals to the number of the measured sizes, $D_{i(j)+1}$ and $A_{i(j)+1}$ can be replaced with the corresponding theoretical critical dry diameter of water ball (Kelvin equation) D_K and the activation ratio of 1. When no measured diameter is smaller than or equals to D_{ij}, $D_{i(j)}$ and $A_{i(j)}$ are replaced with D_{NaCl} and 0, $D_{i(j)+1}$ and $A_{i(j)+1}$ are D_1 and A_1.

With Eq. (A4), Eq. (A1) can be written as

$$M_i = \sum_{j=1}^{J} A_{ij}F_{ij} = \sum_{j=1}^{J}\left(A_{i(j)}P_{ij} + A_{i(j)+1}Q_{ij}\right)F_{ij} = \sum_{i=1}^{I} S_{ij}A_i + T_i, \tag{A5}$$

ACPD
11, 1333–1366, 2011

where S_{ij} and T_i are both expressed as the results of P_{ij}, Q_{ij} and F_{ij}. T_i comes from the terms where $D_{i(j)+1}$ is replaced with Kelvin diameter.

$$S_{ij} = \sum_{j=1}^{J} \left(\delta(i(k),i)P_{ij} + \delta(i(k)+1,i)Q_{ik}\right)F_{ik}. \quad \text{(A6)}$$

$$T_i = \sum_{j=1}^{J} \delta(i(k)+1,i)Q_{ik}F_{ik}. \quad \text{(A7)}$$

A new response is written as $R_i = M_i - T_i$. This equation set is then expressed as

$$\boldsymbol{R} = \mathbf{S}\boldsymbol{A}, \quad \text{(A8)}$$

where $\boldsymbol{R}$ and $\boldsymbol{A}$ are $I \times 1$ vectors and $\mathbf{S}$ is an $I \times I$ matrix. Solving the equation set with non-negative least square method will get the activation ratio of singly changed particles.

Acknowledgements. This work is supported by the National 973 Project of China (2011CB403402), the National Natural Science Foundation of China (NSFC) under grants 40875001, 40975083, 40905060, and the German Science Foundation under grant DFG WI 1449/14-1.

References

Anttila, T.: Sensitivity of cloud droplet formation to the numerical treatment of the particle mixing state, J. Geophys. Res., 115, D21205, doi:10.1029/2010jd013995, 2010.

Bilde, M. and Svenningsson, B.: CCN activation of slightly soluble organics: the importance of small amounts of inorganic salt and particle phase, Tellus B, 56, 128–134, 2004.

Boucher, O. and Lohmann, U.: The sulfate-CCN-cloud albedo effect, Tellus B, 47, 281–300, doi:10.1034/j.1600-0889.47.issue3.1.x, 1995.

Bougiatioti, A., Fountoukis, C., Kalivitis, N., Pandis, S. N., Nenes, A., and Mihalopoulos, N.: Cloud condensation nuclei measurements in the marine boundary layer of the Eastern Mediterranean: CCN closure and droplet growth kinetics, Atmos. Chem. Phys., 9, 7053–7066, doi:10.5194/acp-9-7053-2009, 2009.

ACPD

11, 1333–1366, 2011

Chen, Y., Zhao, C., Zhang, Q., Deng, Z., Huang, M., and Ma, X.: Aircraft study of mountain chimney effect of Beijing, China, J. Geophys. Res., 114, D08306, doi:10.1029/2008jd010610, 2009.
Cooper, J. R. and Dooley, R. B.: IAPWS Secretariat: IAPWS Release on Surface Tension of Ordinary Water Substance, Issued by the International Association for the Properties of Water and Steam, available online at: http://www.iapws.org/relguide/surf.pdf, 1994.
Cruz, C. N. and Pandis, S. N.: A study of the ability of pure secondary organic aerosol to act as cloud condensation nuclei, Atmos. Environ., 31, 2205–2214, 1997.
Deng, Z., Zhao, C., Zhang, Q., Huang, M., and Ma, X.: Statistical analysis of microphysical properties and the parameterization of effective radius of warm clouds in Beijing area, Atmos. Res., 93, 888–896, 2009.
Dusek, U., Frank, G. P., Hildebrandt, L., Curtius, J., Schneider, J., Walter, S., Chand, D., Drewnick, F., Hings, S., Jung, D., Borrmann, S., and Andreae, M. O.: Size matters more than chemistry for cloud-nucleating ability of aerosol particles, Science, 312, 1375–1378, doi:10.1126/science.1125261, 2006.
Facchini, M. C., Mircea, M., Fuzzi, S., and Charlson, R. J.: Cloud albedo enhancement by surface-active organic solutes in growing droplets, Nature, 401, 257–259, 1999.
Frank, G. P., Dusek, U., and Andreae, M. O.: Technical note: A method for measuring size-resolved CCN in the atmosphere, Atmos. Chem. Phys. Discuss., 6, 4879–4895, doi:10.5194/acpd-6-4879-2006, 2006.
Giebl, H., Berner, A., Reischl, G., Puxbaum, H., Kasper-Giebl, A., and Hitzenberger, R.: CCN activation of oxalic and malonic acid test aerosols with the university of Vienna cloud condensation nuclei counter, J. Aerosol Sci., 33, 1623–1634, 2002.
Henning, S., Rosenørn, T., D'Anna, B., Gola, A. A., Svenningsson, B., and Bilde, M.: Cloud droplet activation and surface tension of mixtures of slightly soluble organics and inorganic salt, Atmos. Chem. Phys., 5, 575–582, doi:10.5194/acp-5-575-2005, 2005.
Hori, M., Ohta, S., Murao, N., and Yamagata, S.: Activation capability of water soluble organic substances as CCN, J. Aerosol Sci., 34, 419–448, 2003.
IPCC: Climate Change 2007: The Physical Science Basis, Cambridge University Press, Cambridge, UK and New York, NY, USA, 996 pp., 2007.
Jarvis, A., Reuter, H. I., Nelson, A., and Guevara, E.: Hole-filled seamless SRTM data V4, International Centre for Tropical Agriculture (CIAT), available online: http://srtm.csi.cgiar.org, 2008.

ACPD
11, 1333–1366, 2011

Khvorostyanov, V. I. and Curry, J. A.: Aerosol size spectra and CCN activity spectra: reconciling the lognormal, algebraic, and power laws, J. Geophys. Res., 111, D12202, doi:10.1029/2005jd006532, 2006.
Kulmala, M., Laaksonen, A., Charlson, R. J., and Korhonen, P.: Clouds without supersaturation, Nature, 388, 336–337, 1997.
Kuwata, M., Kondo, Y., Miyazaki, Y., Komazaki, Y., Kim, J. H., Yum, S. S., Tanimoto, H., and Matsueda, H.: Cloud condensation nuclei activity at Jeju Island, Korea in spring 2005, Atmos. Chem. Phys., 8, 2933–2948, doi:10.5194/acp-8-2933-2008, 2008.
Lance, S., Medina, J., Smith, J. N., and Nenes, A.: Mapping the operation of the dmt continuous flow CCN counter, Aerosol Sci. Tech., 40, 242–254, 2006.
Liu, P., Zhao, C., Zhang, Q., Deng, Z., Huang, M., Ma, X., and Tie, X.: Aircraft study of aerosol vertical distributions over Beijing and their optical properties, Tellus B, 61, 756–767, 2009.
Liu, P. F., Zhao, C. S., Göbel, T., Hallbauer, E., Nowak, A., Ran, L., Xu, W. Y., Deng, Z. Z., Ma, N., Mildenberger, K., Henning, S., Stratmann, F., and Wiedensohler, A.: Hygroscopic properties of aerosol particles at high relative humidity and their diurnal variations in the North China plain, to be submitted to Atmos. Chem. Phys. Discuss., submitted, 2011.
Low, R. D. H.: A generalized equation for the solution effect in droplet growth, J. Atmos. Sci., 26, 608–611, 1969.
Medina, J., Nenes, A., Sotiropoulou, R.-E. P., Cottrell, L. D., Ziemba, L. D., Beckman, P. J., and Griffin, R. J.: Cloud condensation nuclei closure during the international consortium for atmospheric research on transport and transformation 2004 campaign: Effects of size-resolved composition, J. Geophys. Res., 112, D10S31, doi:10.1029/2006jd007588, 2007.
Moore, R. H., Nenes, A., and Medina, J.: Scanning mobility CCN analysis – a method for fast measurements of size-resolved CCN distributions and activation kinetics, Aerosol Sci. Tech., 44, 861–871, 2010.
Roberts, G. C. and Nenes, A.: A continuous-flow streamwise thermal-gradient CCN chamber for atmospheric measurements, Aerosol Sci. Tech., 39, 206–221, 2005.
Rogers, R. R. and Yau, M. K.: A short course in cloud physics, 3rd edn., Pergamon Press, 293 pp., 1989.
Rose, D., Gunthe, S. S., Mikhailov, E., Frank, G. P., Dusek, U., Andreae, M. O., and Pöschl, U.: Calibration and measurement uncertainties of a continuous-flow cloud condensation nuclei counter (DMT-CCNC): CCN activation of ammonium sulfate and sodium chloride aerosol particles in theory and experiment, Atmos. Chem. Phys., 8, 1153–1179, doi:10.5194/acp-8-

ACPD
11, 1333–1366, 2011

1153-2008, 2008.
Rose, D., Nowak, A., Achtert, P., Wiedensohler, A., Hu, M., Shao, M., Zhang, Y., Andreae, M. O., and Pöschl, U.: Cloud condensation nuclei in polluted air and biomass burning smoke near the mega-city Guangzhou, China – Part 1: Size-resolved measurements and implications for the modeling of aerosol particle hygroscopicity and CCN activity, Atmos. Chem. Phys., 10, 3365–3383, doi:10.5194/acp-10-3365-2010, 2010.
Seinfeld, J. H. and Pandis, S. N.: Atmospheric Chemistry and Physics: From Air Pollution to Climate Change, 2 edn., John Wiley & Sons, Inc., 1225 pp., 2006.
Stroud, C. A., Nenes, A., Jimenez, J. L., DeCarlo, P. F., Huffman, J. A., Bruintjes, R., Nemitz, E., Delia, A. E., Toohey, D. W., Guenther, A. B., and Nandi, S.: Cloud activating properties of aerosol observed during celtic, J. Atmos. Sci., 64, 441–459, 2007.
Su, H., Rose, D., Cheng, Y. F., Gunthe, S. S., Massling, A., Stock, M., Wiedensohler, A., Andreae, M. O., and Pöschl, U.: Hygroscopicity distribution concept for measurement data analysis and modeling of aerosol particle mixing state with regard to hygroscopic growth and CCN activation, Atmos. Chem. Phys., 10, 7489–7503, doi:10.5194/acp-10-7489-2010, 2010.
Twomey, S.: The nuclei of natural cloud formation part ii: The supersaturation in natural clouds and the variation of cloud droplet concentration, Pure Appl. Geophys., 43, 243–249, 1959.
Wiedensohler, A.: An approximation of the bipolar charge distribution for particles in the submicron size range, J. Aerosol Sci., 19, 387–389, 1988.
Wiedensohler, A., Cheng, Y. F., Nowak, A., Wehner, B., Achtert, P., Berghof, M., Birmili, W., Wu, Z. J., Hu, M., Zhu, T., Takegawa, N., Kita, K., Kondo, Y., Lou, S. R., Hofzumahaus, A., Holland, F., Wahner, A., Gunthe, S. S., Rose, D., Su, H., and Pöschl, U.: Rapid aerosol particle growth and increase of cloud condensation nucleus activity by secondary aerosol formation and condensation: a case study for regional air pollution in Northeastern China, J. Geophys. Res., 114, D00G08, doi:10.1029/2008jd010884, 2009.
Wiedensohler, A., Birmili, W., Nowak, A., Sonntag, A., Weinhold, K., Merkel, M., Wehner, B., Tuch, T., Pfeifer, S., Fiebig, M., Fjäraa, A. M., Asmi, E., Sellegri, K., Depuy, R., Venzac, H., Villani, P., Laj, P., Aalto, P., Ogren, J. A., Swietlicki, E., Roldin, P., Williams, P., Quincey, P., Hüglin, C., Fierz-Schmidhauser, R., Gysel, M., Weingartner, E., Riccobono, F., Santos, S., Grüning, C., Faloon, K., Beddows, D., Harrison, R. M., Monahan, C., Jennings, S. G., O'Dowd, C. D., Marinoni, A., Horn, H.-G., Keck, L., Jiang, J., Scheckman, J., McMurry, P. H., Deng, Z., Zhao, C. S., Moerman, M., Henzing, B., and de Leeuw, G.: Particle mobility size

ACPD
11, 1333–1366, 2011

spectrometers: harmonization of technical standards and data structure to facilitate high quality long-term observations of atmospheric particle number size distributions, Atmos. Meas. Tech. Discuss., 3, 5521–5587, doi:10.5194/amtd-3-5521-2010, 2010.

Xu, W. Y., Zhao, C. S., Ran, L., Deng, Z. Z., Liu, P. F., Ma, N., Lin, W. L., Xu, X. B., Yan, P., He, X., Yu J., Liang, W. D., and Chen, L. L.: Characteristics of pollutants and their correlation to meteorological conditions at a suburban site in the North China Plain, Submitted to Atmos. Chem. Phys. Discuss., submitted, 2011.

Young, K. C. and Warren, A. J.: A reexamination of the derivation of the equilibrium supersaturation curve for soluble particles, J. Atmos. Sci., 49, 1138–1143, 1992.

Zhao, C., Ishizaka, Y., and Peng, D.: Numerical study on impacts of multi-component aerosols on marine cloud microphysical properties, J. Meteorol. Soc. Jp., 83, 977–986, 2005.

Zhao, C., Tie, X., and Lin, Y.: A possible positive feedback of reduction of precipitation and increase in aerosols over Eastern Central China, Geophys. Res. Lett., 33, L11814, doi:10.1029/2006gl025959, 2006.

ACPD

11, 1333–1366, 2011

Table 1. Critical dry diameter of NaCl, $(NH_4)_2SO_4$ and an insoluble but wettable (IBW) substance.

SS (%)	Critical Dry Diameter (nm)		
	NaCl	$(NH_4)_2SO_4$	IBW
0.05	162	204	4206
0.07	129	164	3004
0.10	102	130	2103
0.20	65	83	1052
0.30	49	64	702
0.40	41	53	527
0.50	35	46	422
0.60	31	41	351
0.70	28	37	301
0.80	26	34	264
0.90	24	31	235
1.00	22	29	211

ACPD
11, 1333–1366, 2011

Table 2. Statistics of the aerosol number concentration and CCN number concentration.

	0.056%	0.083%	0.17%	0.35%	0.70%	N_a
Min	76	142	482	1115	1840	1924
Max	6084	7135	11 539	21 151	28 488	59 003
Mean	2192	2957	5977	10 279	12 963	14 651
Std	1653	2012	3135	4879	5725	7483
N	930	934	931	926	921	5453

The N_{CCN} (cm^{-3}) at five supersaturations and the aerosol number concentration (N_a, cm^{-3}) are presented. The minimum, maximum, mean value and the corresponding standard deviation are presented. The last line is the number of samples.

ACPD
11, 1333–1366, 2011

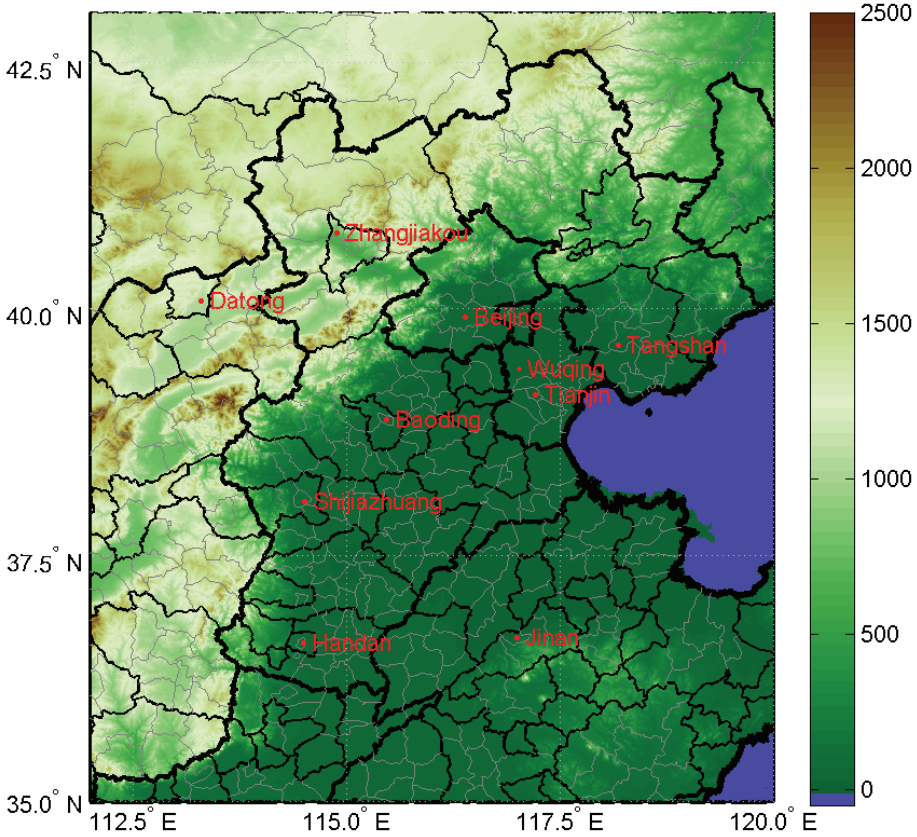

Fig. 1. The map for the measurement site. The color represents the elevation with data from Jarvis et al. (2008). The main cities in this area are marked in the map.

ACPD
11, 1333–1366, 2011

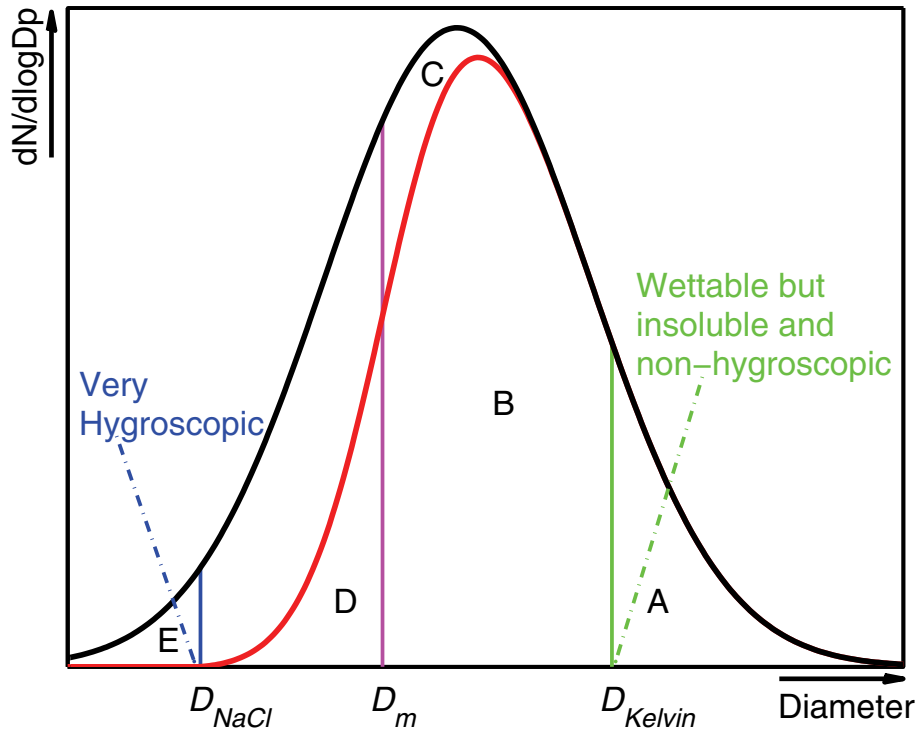

Fig. 2. Schematic of the relationship between aerosol and CCN. The black curve represents the aerosol size distribution, while only the particles under the red curve act as CCN. D_m is regarded as an inferred critical dry diameter at the given SS. The number concentration of the aerosols larger than D_m equals to the N_{CCN}. D_{NaCl} is the critical dry diameter of NaCl particle at the given SS. D_{Kelvin} is the critical diameter for an insoluble but wettable particle (IBW) at the given SS. All the aerosol particles with diameter larger than D_{Kelvin} (area A) can be activated, while the atmospheric aerosol particles smaller than D_{NaCl} (area E) cannot be activated. The area C and D equals to each other.

ACPD
11, 1333–1366, 2011

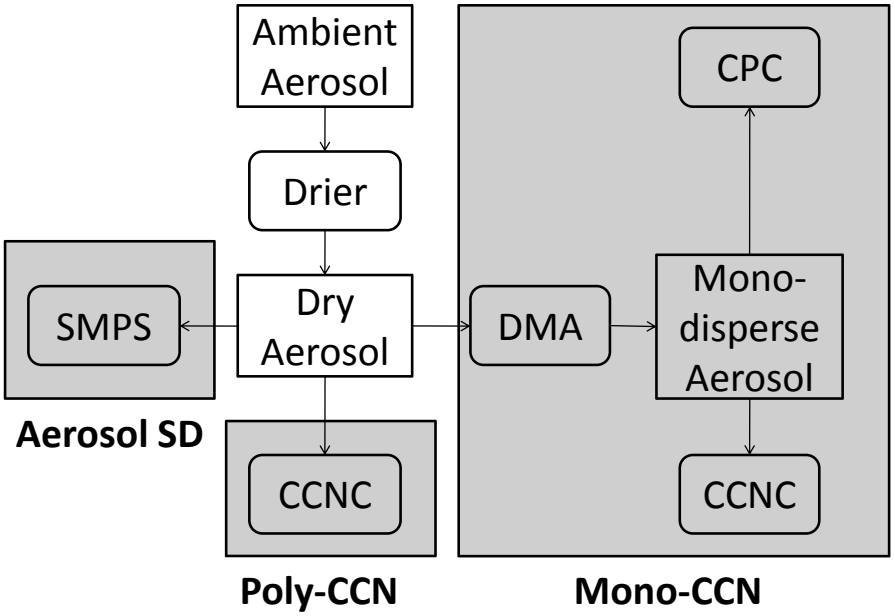

Fig. 3. Instrumentation set-up.

ACPD
11, 1333–1366, 2011

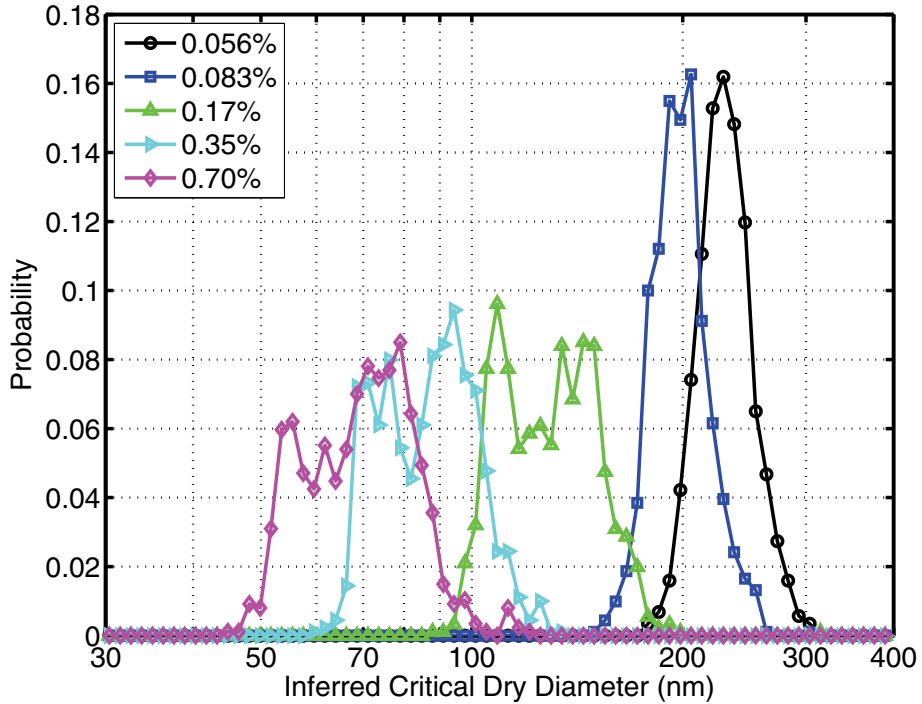

Fig. 4. Probability distribution of the inferred critical dry diameter.

ACPD
11, 1333–1366, 2011

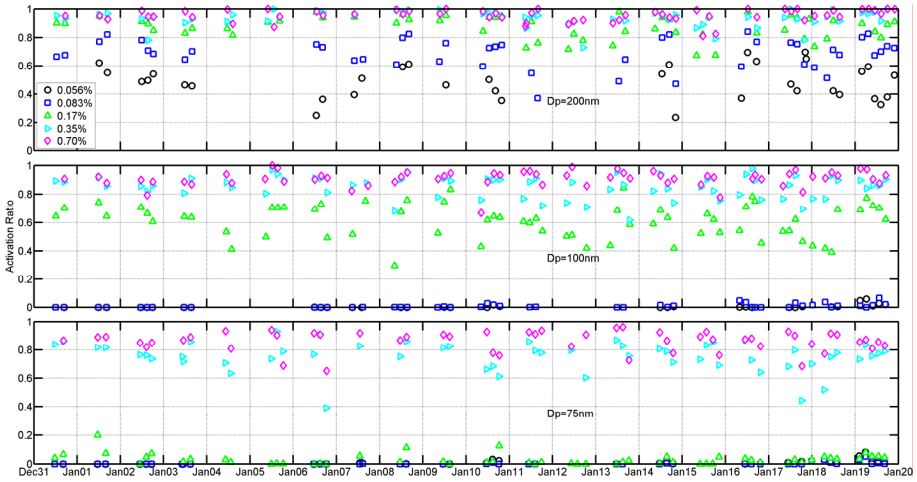

Fig. 5. Time series of the activation ratio during January 2010.

ACPD
11, 1333–1366, 2011

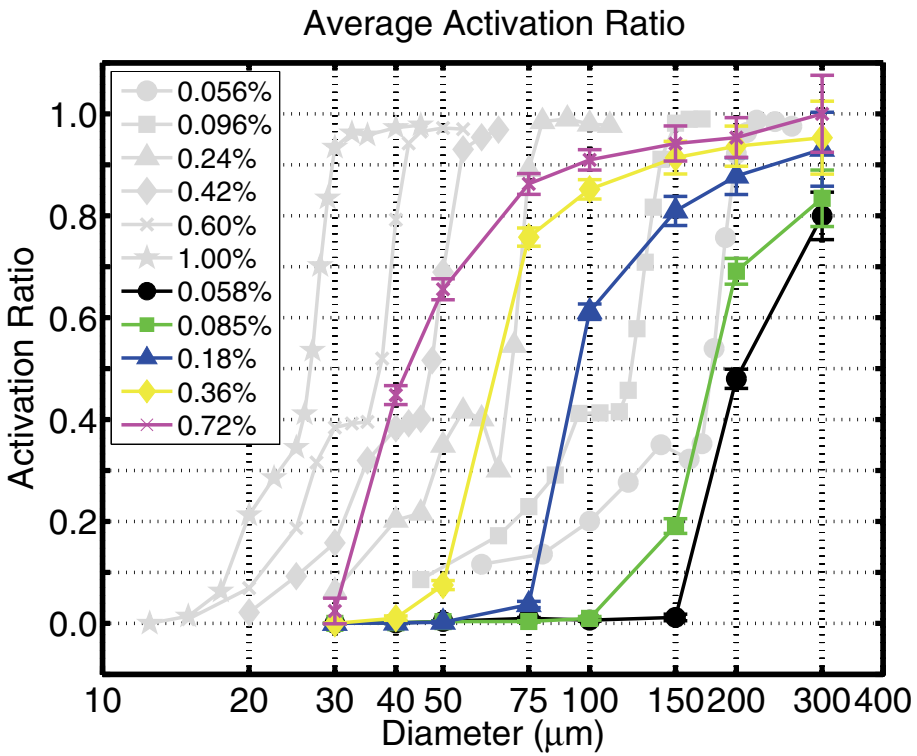

Fig. 6. The average activation curve for different supersaturations. Calibration curve of ammonia sulfate particles are shown as gray curves labeled with the effective supersaturation. The colored curves are the average activation curves of ambient aerosols.

ACPD
11, 1333–1366, 2011

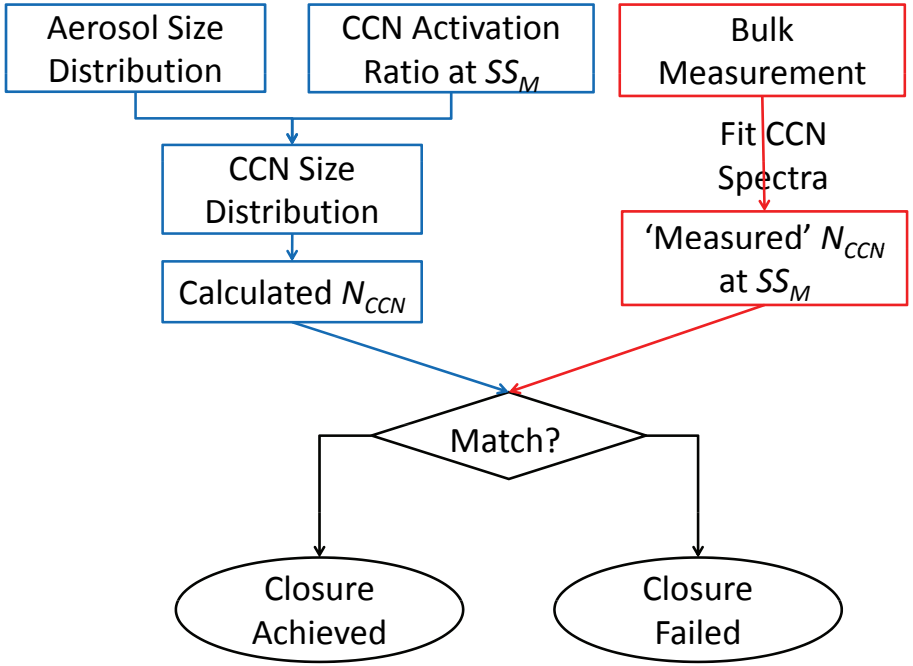

Fig. 7. The flowchart for CCN closure between bulk and size-resolved measurement.

ACPD
11, 1333–1366, 2011

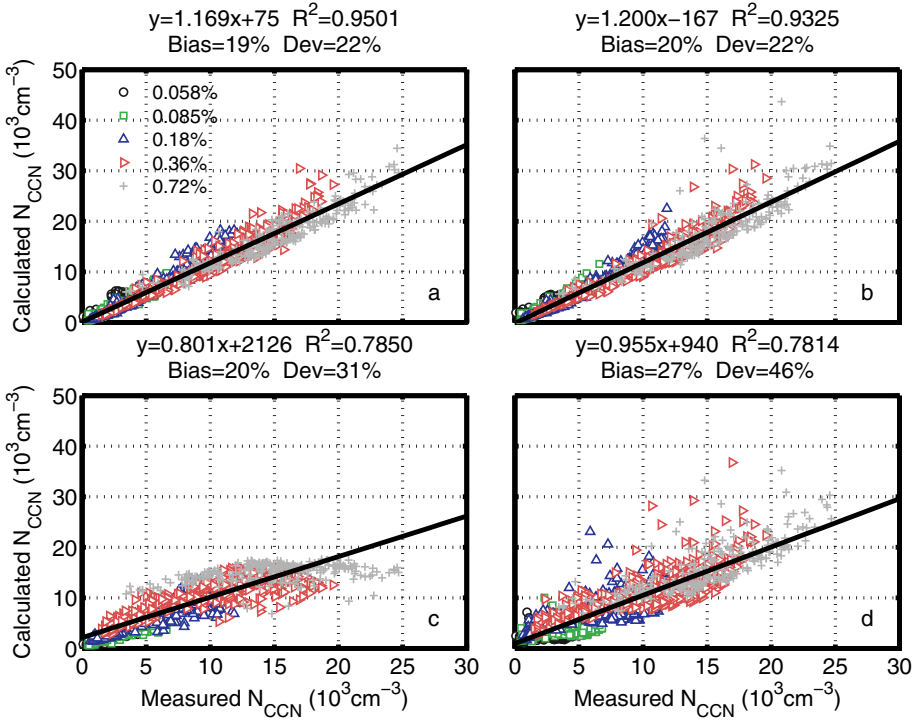

Fig. 8. Closure between measured CCN number concentration and the CCN number concentration calculated from aerosol number size distribution (SD) and size-resolved activation ratio (SRAR) for different supersaturations. **(a)** Real-time SD and SRAR; **(b)** Real-time SD and Averaged SRAR; **(c)** Average Na (keep NASD) and Real-time SRAR; d: Average NASD (keep Na) and Real-time SRAR. There are 1527 pairs of data in each panel. The title of each panel shows the fitted function, correlation coefficient, average relative bias (Bias=$(N_{CCN,cal}-N_{CCN,m})/N_{CCN,m}$) and average relative deviation (Dev=$|N_{CCN,cal}-N_{CCN,m}|/N_{CCN,m}$).

ACPD
11, 1333–1366, 2011